Aerosol and Air Quality Research, 14: 500–514, 2014

ISSN: 1680-8584 print / 2071-1409 online
doi: 10.4209/aaqr.2013.05.0169

Towards Solar Thermochemical Carbon Dioxide Capture via Calcium Oxide Looping: A Review

Leanne Reich[1], Lindsey Yue[1], Roman Bader[2], Wojciech Lipiński[2*]

[1] *Department of Mechanical Engineering, University of Minnesota, 111 Church Street SE, Minneapolis, Minnesota 55455, USA*
[2] *Research School of Engineering, Australian National University, Canberra, ACT 0200, Australia*

ABSTRACT

This article presents a review of research in the field of solar thermochemical carbon dioxide capture based on calcium oxide looping. Topics covered include thermodynamics, kinetics, and heat and mass transfer as well as reactor design, modeling, and testing.

Keywords: Calcination; Carbonation; Chemical looping; Solar reactor; Solar energy.

INTRODUCTION

Carbon dioxide (CO_2) makes up 77% of all greenhouse gas emissions worldwide and 80% in the United States, primarily due to the use of fossil fuels as the source of energy (U.S. Energy Information Administration, 2009). Worldwide energy use continues to grow at a rate of about 1.6% per year, and 87% of that energy comes from fossil fuel sources (BP Statistical Review of World Energy, 2012; U.S. Energy Information Administration, 2011). At the same time, CO_2 is a valuable commodity with applications in the pharmaceutical, medical, environmental, food and beverages, petrochemical, oil recovery, metallurgy, and manufacturing industries (Stalkup, 1978; Pierantozzi, 2003). In 2005, industrial CO_2 use was estimated to be 6.3 Gt-CO_2/yr (Metz *et al.*, 2005). An emerging use of CO_2 is for the solar-driven production of synthesis gas, which in turn can be used to obtain synthetic hydrocarbon fuels (Steinfeld *et al.*, 1998; Chueh *et al.*, 2005; Leckel, 2009; Hathaway *et al.*, 2011). Employment of CO_2 capture systems may become necessary in the near future to stabilize CO_2 concentration in the atmosphere if the world continues to rely on fossil fuels for energy production. Such systems can also become a key technical solution to close the anthropogenic carbon cycle in a renewable-based energy system involving solar-derived hydrocarbon fuels as the primary chemical energy carriers.

The theoretical minimum energy required to capture CO_2 is set by the reversible separation work of a binary CO_2-containing gas mixture, given by

$$\overline{W}_{\min} = -\frac{\overline{R}T}{1000}\frac{\bar{x}\ln(\bar{x}) + (1-\bar{x})\ln(1-\bar{x})}{\bar{x}} \quad (1)$$

where $\overline{W}_{\min}$ is the minimum work of separation in kJ per mole of gas separated, $\overline{R}$ is the universal gas constant, T is the temperature, and $\bar{x}$ is the mole fraction of the gas being separated from the mixture (Kalafati, 1991). $\overline{W}_{\min}$ is shown in Fig. 1 as a function of mole fraction of CO_2 in the binary mixture. At CO_2 molar fractions below 8×10^{-4} the work required is over 20 kJ/mol$_{CO_2}$ and decreases to 7 kJ/mol$_{CO_2}$ at a CO_2 molar fraction of 0.15.

Many carbon dioxide capture technologies have been investigated to date, including pre-combustion capture, post-combustion capture, oxycombustion, and capture from industrial processes (Metz *et al.*, 2005). Methods used by capture technologies include physical or chemical absorption, adsorption, membrane separation, and cryogenic separation (Rackley, 2010). Absorption technologies have been in commercial use for over 50 years but have only recently been applied to low concentrations of CO_2 such as those found in exhaust gases. Commonly used solvents and sorbents in chemical absorption capture are amines, carbonates, and aqueous ammonia. Monoethanolamine (MEA) is the most common solvent used in commercial applications (Wilson and Gerard, 2007). Some solvents used in physical absorption are methanol, propylene carbonate, and dimethyl ethers of polyethylene glycol. Some disadvantages to absorption capture are the high amount of energy required to regenerate the solvent, degradation of the solvent by other components of flue gas such as particulates, SO_x and NO_x, and decreased

* Corresponding author.
Tel.: +61-2-61-25-7896
E-mail address: wojciech.lipinski@anu.edu.au

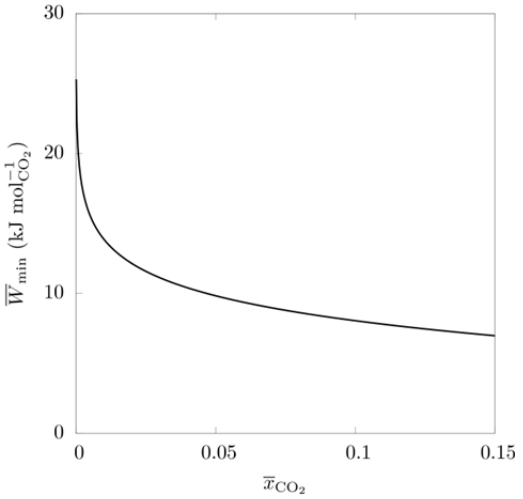

Fig. 1. Thermodynamic minimum separation work of a binary gas mixture (Matthews and Lipiński, 2012). Reproduced with permission from Elsevier.

reactivity of the solvent with successive cycles (Chapel *et al.*, 1999; Aaron and Tsouris, 2005). Chemical sorbents for CO_2 capture by adsorption include various metal oxides and solid amines. Physical sorbents in use include activated carbon, activated alumina, and silica gel (Rackley, 2010). The main disadvantages to adsorption are low reaction rates and reduced effectiveness at CO_2 concentrations higher than 0.04 to 1.5% (IEA Greenhouse Gas R&D Programme, 1994). In membrane separation, the membrane essentially works as a filter, separating out CO_2 from the rest of the gas flow (Aaron and Tsouris, 2005). There are many materials used as membranes, but they can generally be divided into the categories of porous and nonporous. The main disadvantages to membrane separation are higher energy requirements, lower percentage of CO_2 removed than a chemical absorption based process, and reduced effectiveness at lower CO_2 concentrations (IEA Greenhouse Gas R&D Programme, 1994). Cryogenic separation relies on the difference in boiling points of the exhaust gas constituents. Cryogenic separation of CO_2 is typically used in the production of sales-quality natural gas. The main disadvantage to cryogenic separation of CO_2 is the large energy cost associated with cooling the gases (Aaron and Tsouris, 2005). The costs of each type of capture vary greatly depending on the specific situation. For example, Tuinier *et al.* (2011) state that cryogenic capture is favorable when low cost liquefied natural gas (LNG) is available, absorption is favorable when low cost steam is available, and membrane separation has advantages when neither LNG nor steam are cheaply available. As noted in Metz *et al.* (2005), the majority of carbon capture technologies are in the development stage, so costs are estimated based on analysis of hypothetical power plants. The sensitivity of these analyses to assumptions makes it difficult to draw firm conclusions about cost when comparing different studies.

One chemical absorption approach to CO_2 capture, often referred to as CaO–$CaCO_3$ looping, uses calcium oxide (CaO) carbonation combined with calcium carbonate ($CaCO_3$) calcination:

Carbonation step (exothermic):

$$CaO + CO_2 \rightarrow CaCO_3, \quad \Delta\overline{h}^0_{298K} = -178 \text{ kJ/mol} \tag{2a}$$

Calcination step (endothermic):

$$CaCO_3 \rightarrow CaO + CO_2, \quad \Delta\overline{h}^0_{298K} = 178 \text{ kJ/mol} \tag{2b}$$

$\Delta\overline{h}^0_{298K}$ is the molar reaction enthalpy change at 298 K. A 3 step cycle involving hydration of CaO to form calcium hydroxide, $Ca(OH)_2$, has also been proposed to avoid the kinetic limitations of the CaO-carbonation reaction:

Hydration step (exothermic):

$$CaO + H_2O \rightarrow Ca(OH)_2, \quad \Delta\overline{h}^0_{298K} = -65 \text{ kJ/mol} \tag{3a}$$

Carbonation step (exothermic):

$$Ca(OH)_2 + CO_2 \rightarrow CaCO_3 + H_2O, \quad \Delta\overline{h}^0_{298K} = -109 \text{ kJ/mol} \tag{3b}$$

Calcination step (endothermic):

$$CaCO_3 \rightarrow CaO + CO_2, \quad \Delta\overline{h}^0_{298K} = 178 \text{ kJ/mol} \tag{3c}$$

The cycles (2a)–(2b) and (3a)–(3c) operate at low pressures, can capture more CO_2 per unit mass of sorbent than other processes, and use CaO as a low cost sorbent that is obtained from natural limestone and dolomite (Gupta and Fan, 2002; Abanades *et al.*, 2004a). A challenge for realizing the CaO carbonation-calcination cycles is the high temperature required for the calcination step, typically achieved via combustion of fossil fuels. An alternative to combustion is to employ concentrated solar energy as the high-temperature source of process heat. The latter approach allows mitigation of additional CO_2 emissions associated with the generation of the process heat. The use of concentrated solar radiation has been proposed to drive numerous high-temperature processes, which can potentially run continuously if coupled with thermal storage (Fletcher, 2001; Steinfeld and Palumbo, 2001; Kodama and Gokon, 2007).

CO_2 capture using a CaO based cycle was investigated by Shimizu *et al.* (1999). A pair of conceptual fluidized beds connected by solid transport pipes and attached to a 1000 MW air-fired coal power plant was studied. The carbonation temperature was 873 K and the calcination temperature was 1223 K. Heat was recovered from the exothermic carbonation reaction and the cooling stream of CO_2 using a secondary steam cycle. Use of heat recovery boosted the plant efficiency to 33.4% compared to 32% for an oxygen-fired coal plant with heat recovery.

An 18 kW pilot scale batch mode fluidized bed for the CaO carbonation–calcination cycle studied by Abanades *et al.* (2004b) is shown in Fig. 2. The fluidized bed was shown to be effective for CO_2 capture at a temperature near 650°C. The carbonation reaction was fast enough at atmospheric

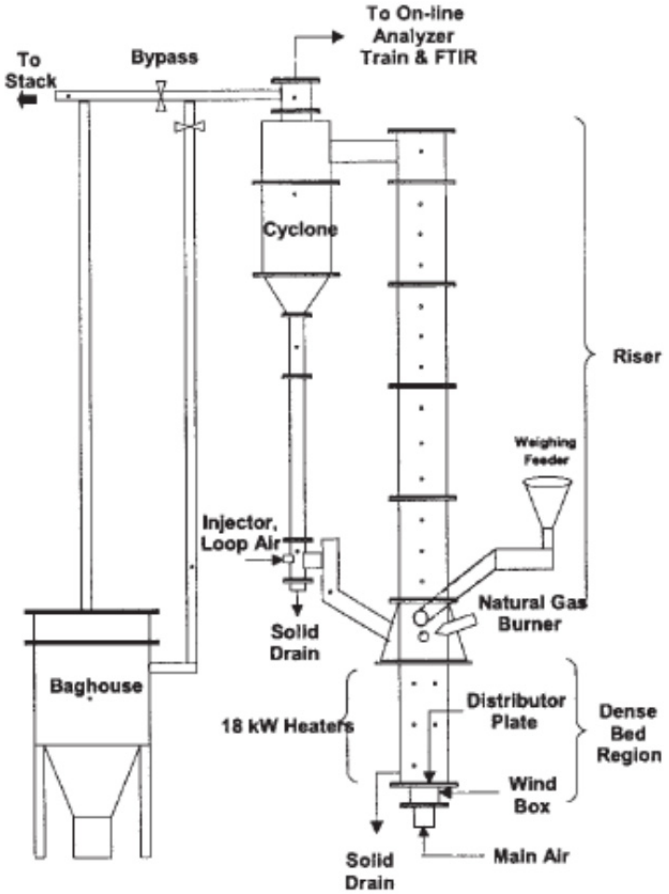

Fig. 2. Pilot scale fluidized-bed carbonator (Abanades *et al.*, 2004b). Reproduced with permission from John Wiley and Sons.

pressure to completely remove CO_2 from the input gas at a bed height of 0.25 m. The reactivity of the CaO decreased with an increased number of cycles, although the rate of decay and the residual conversion depended on the type of limestone used. Havelock limestone behaved similarly to limestone in other studies and performed better than Cadomin limestone.

A 75 kW pilot scale dual fluidized bed setup was investigated by Lu *et al.* (2008). It was the first to feature a continuous cycle utilizing two beds rather than a batch cycle where carbonation and calcination occurred in the same location. Cyclones collected particles from the top of the carbonator and cycled them to the calciner and vice versa. The solids flow was controlled by solenoid valves. CO_2 concentration entering the carbonator was nominally 15%. Heat was supplied to the calciner by electric heaters or by burning biomass or coal. The calcination temperature ranged from 850 to 950°C and the carbonation temperature ranged from 580 to 720°C. During the first 10 cycles, the fraction of CO_2 removed from the inlet gas, was greater than 90%, and it decreased to approximately 70% after 25 cycles. Increasing the carbonation temperature improved the efficiency in later cycles. The authors speculated that this is due to particle sintering and pore plugging blocking the ability for CO_2 to reach deep pores after cycling of the sorbent.

Several other laboratory scale dual fluidized bed setups have been investigated, and three were summarized by Rodriguez *et al.* (2011). The facilities were 10–75 kW dual fluidized beds operating in several regimes of fluidization. Carbonation temperatures ranged from 600–700°C and calcination temperatures ranged from 800–900°C. Two of the facilities operated continuously while the other was semi-continuous. The semi-continuous setup allowed for the effect of cycling to be observed at the expense of achieving steady state, while the continuous setups contained a mixture of particles with different histories but could achieve steady state operation. Each facility used different fuel and limestone sources, but all achieved CO_2 capture efficiencies above 70%, demonstrating that CO_2 capture using fluidized beds is industrially viable for a wide range of conditions.

To date, researchers have demonstrated that CO_2 capture via the CaO carbonation-calcination cycle is a feasible method. It has been shown that fluidized beds are suitable for the process because they provide favorable heat and mass transfer conditions in the reactor and can be scaled up as needed. However, while there has been a large body of research conducted regarding CO_2 capture with CaO using fossil energy, using concentrated solar energy to drive the cycle is a relatively new concept. This paper presents a review of past work on CaO-based CO_2 capture, with a particular focus on the use of solar energy to drive the process. Thermodynamic analyses of the cycles are

discussed, followed by particle level studies of kinetics and heat and mass transfer. The paper concludes with a summary of reactor level design, modeling, and experiments.

THERMODYNAMIC ANALYSES

Nikulshina *et al.* (2006) performed a thermodynamic analysis for CO_2 capture from atmospheric air using the three step carbonation cycle (3a)–(3c). The model system is shown in Fig. 3. Calcium hydroxide was carbonated with atmospheric air containing 500 ppm CO_2 at 500 K, the resulting $CaCO_3$ calcined at 1500 K to form CaO, and finally slaked at 353 K to form $Ca(OH)_2$. Assumptions made included ideal heat exchange, adiabatic carbonation, pure substances, and chemical equilibrium. Pumping work was not included in the analysis. The total heat required for the cycle without heat recovery was 12.1 MJ/mol_{CO_2} captured. The addition of two heat exchangers to recover heat from the CO_2-depleted air exiting the carbonator and the CO_2 exiting the calciner reduced the heat requirement to 2.5 MJ/mol_{CO_2} captured.

Rodriguez *et al.* (2008) examined the heat requirements in a coal fired calciner as a function of carbonation conversion, coal composition, and sorbent makeup flow. At a residual carbonation conversion of 0.075 and no makeup flow of sorbent, the heat requirement for the calciner was 36.9% of the plant input. Assuming a 1 mol_{CO_2}/s capture rate and using the study data this translates to about 3.9 MJ/mol_{CO_2} captured.

Martinez *et al.* (2012) examined the effects of adding solid heat recovery to the cycle (2a)–(2b) by simulating four different solid heat exchange configurations. Indirect solid heat exchange between hot CaO and cool $CaCO_3$ was the most efficient option, increasing thermal efficiency by up to 2% compared to a case with no solid heat recovery. A solid heat exchange system with a mixing seal valve showed no improvement compared to the base case. A system with a heat recovery fluidized bed preheating $CaCO_3$ with hot CO_2 increased thermal efficiency by up to 1.4%.

A thermodynamic analysis of the cycle (2a)–(2b) was performed to determine the effect of input CO_2 concentration, reaction temperatures, and gas and solid phase heat recovery on the total solar energy required (Matthews and Lipiński, 2012). The system used for the analysis is shown in Fig. 4. Input gas at T_0 containing a variable amount of CO_2 was preheated by CO_2-depleted gas exiting the carbonator, CO_2 exiting the calciner, and the exothermic carbonation reaction before entering the carbonator at T_3. CO_2 in the input gas reacted with CaO to form $CaCO_3$ at T_{carb}. $CaCO_3$ exited the carbonator and was preheated by CaO and CO_2 exiting the calciner. In the calciner, concentrated solar energy provided heat for the endothermic calcination reaction at T_{calc}. CaO and CO_2 exited the calciner and were used for preheating before the cycle began again. Chemical equilibrium was assumed for each reaction and any heat not recovered was rejected to the environment.

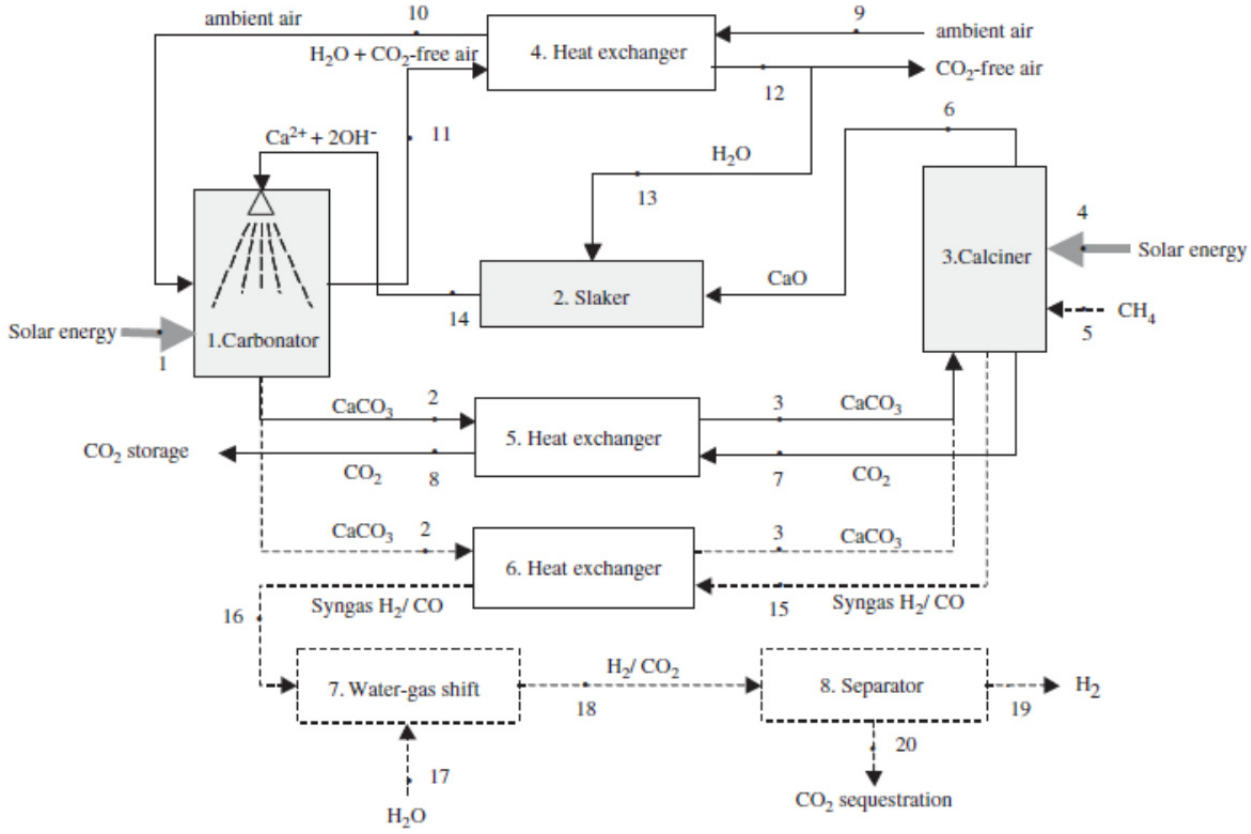

Fig. 3. Cycle for CO_2 capture from air including a slaker. Solid lines indicate a CO_2 capture only cycle and dotted lines indicate a cycle that co-produces hydrogen (Nikulshina *et al.*, 2006). Reproduced with permission from Elsevier.

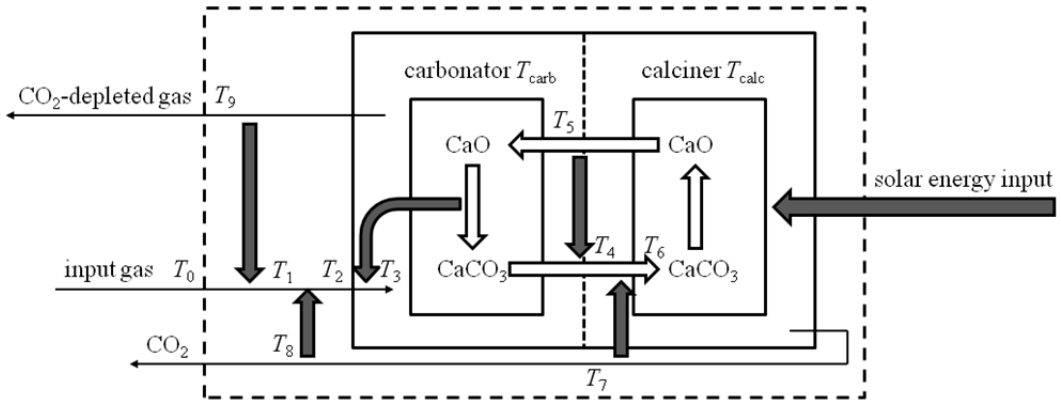

Fig. 4. Cycle for CO_2 capture with gas and solid heat recovery (Matthews and Lipiński, 2012). Reproduced with permission from Elsevier.

The required solar energy for a carbonation temperature of 673 K and a calcination temperature of 1273 K was greater than 45 $MJ/mol_{CO_2\ captured}$ for a CO_2 concentration of 300 ppm and no heat recovery. The minimum value of $\bar{Q}_{solar}$ for 100% solid heat recovery and 0% gas heat recovery was 303 $kJ/mol_{CO_2\ captured}$. $\bar{Q}_{solar}$ for 100% gas heat recovery and 0% solid heat recovery was 283 $kJ/mol_{CO_2\ captured}$. $\bar{Q}_{solar}$ for 100% gas and solid heat recovery was 207 $kJ/mol_{CO_2\ captured}$. Gas heat recovery was more important at low CO_2 input concentrations because of the large amount of inert gas that must be heated to the carbonation temperature. At higher CO_2 input concentrations near 15%, solid heat recovery became nearly as important as gas heat recovery. Gas heat recovery could reduce the required solar energy by 22–99% and solid heat recovery could reduce the required solar energy by 0.1–26%.

These thermodynamic analyses have demonstrated the need for heat recovery in CaO-looping based CO_2 capture systems to reduce the energy requirements and thus the overall cost of using such systems on an industrial scale. Gas heat recovery has a larger potential to reduce energy requirements, but non-negligible reduction can also be obtained by implementing solid heat recovery at higher CO_2 concentrations in the input gas stream such as that produced by a combustion-based power plant.

KINETIC ANALYSES

Calcination Kinetics

The kinetics of the calcination reaction have been extensively studied. Borgwardt (1985) studied the kinetics of the calcination of two different limestone types with particle diameters ranging from 1 to 90 μm using a differential reactor. At 850°C, the reaction was first order with respect to $CaCO_3$ surface area with a rate constant of 1.6×10^{-6} $mol/cm^2/s$. The activation energy was 205 kJ/mol. The calcination reaction conversion as a function of time at a reaction temperature of 720°C is shown in Fig. 5. Dennis and Hayhurst (1987) found the rate constant to be 1.0×10^{-6} $mol/cm^2/s$ and the activation energy to be 169 kJ/mol at the same temperature, but noted that the rate was a function of both CO_2 partial pressure and total pressure.

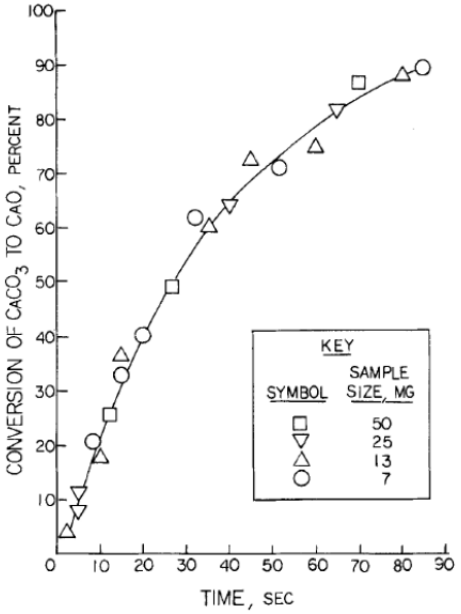

Fig. 5. Calcination conversion as a function of time at 720°C (Borgwardt, 1985). Reproduced with permission from John Wiley and Sons.

They also found that the reaction was chemically controlled and that increasing the total pressure increased the reaction time regardless of CO_2 partial pressure. Escardino *et al.* (2008) summarized the results of several studies from 1930–1974, noting that the reported reaction order varied from 0 to 1 and the reported activation energy varied from 147 to 397 kJ/mol. Their own study resulted in an activation energy of 175 kJ/mol and a reaction order of 1/3. Garcia-Labiano *et al.* (2002) studied the calcination reaction using several sources of limestone. They found that the pre-exponential factor of the Arrhenius equation ranged from 29.5 to 6.7×10^6 $mol/cm^2/s$ and that the activation energy ranged from 114 to 166 kJ/mol depending on the sorbent source. Acharya *et al.* (2012) studied the calcination reaction in atmospheres of N_2, steam, and CO_2. They found that the pre-exponential factor ranged from 2.12–4.82 $\times 10^{10}$ s^{-1} and that activation energy ranged from 180 to 257 kJ/mol.

The N_2 atmosphere had the highest pre-exponential factor and activation energy and the CO_2 atmosphere had the lowest. A summary of rate equations for the calcination reaction is shown in Table 1.

Carbonation Kinetics

The kinetics of the carbonation reaction have also been widely studied. The reaction is generally considered to be chemically controlled initially and switches to a diffusion controlled regime due to formation of a $CaCO_3$ product layer. Bhatia and Perlmutter (1983) found the reaction rate constant to be an average of 0.0595 cm^4/mol/s for temperatures ranging from 550 to 725°C and gas atmospheres containing 2 to 10% CO_2. Shimizu *et al.* (1999) found the reaction rate to be first order with respect to CO_2 concentration, but the maximum conversion decreased as the CaO was cycled. The reaction rate constant was unaffected by cycling and had an average value of 25 m^3/kmol/s for reaction atmospheres containing 5 to 15% CO_2. Fang *et al.* (2009) found the rate constant to be 2.1 × 10^{-3} m^3/mol/s for the chemically controlled initial reaction and 2.5 × 10^{-3} m^3/mol/s for the diffusion controlled regime for a reaction atmosphere of 20% CO_2. A summary of rate equations for the carbonation reaction is shown in Table 2.

Nikulshina *et al.* (2007) conducted a thermogravimetric (TG) analysis of the carbonation of CaO and $Ca(OH)_2$ using atmospheric levels of CO_2. The CaO carbonation reaction rate was chemically controlled initially and switched to a diffusion controlled regime after 20 minutes due to formation of a $CaCO_3$ product layer. The CaO reaction $n_{CaO,0}$, is shown in Fig. 6(a). The final reaction extent at 100 minutes ranged from 0.008 at 300°C to 0.05 at 450°C. Above 450°C, the calcination reaction began to become favorable, so the final reaction extent decreased above this temperature. The reaction rate of $Ca(OH)_2$ carbonation did not switch regimes with time, instead demonstrating diffusion controlled kinetics below 350°C and chemically controlled kinetics above 350°C. The $Ca(OH)_2$ reaction extent as a function of time is shown in Fig. 6(b). The $Ca(OH)_2$ had a higher final reaction extent of 0.25 after 100 minutes at 425°C. The experimental data for CaO was fitted using an unreacted core model and the data for $Ca(OH)_2$ was fitted using a kinetic model accounting for the formation of an interface of water or OH^- ions. Numerical modeling results are shown in Figs. 6(a) and 6(b) with solid lines.

Sorbent Degradation

Degradation of the CaO sorbent over the course of multiple cycles has been identified as a limiting factor in the use of the cycle for CO_2 capture. Abanades (2002) proposed a model for carbonation conversion over a number of cycles:

$$X_{c,N} = f^{N+1} + b \tag{4}$$

where $X_{c,N}$ is the carbonation conversion at the end of the chemically controlled portion of the carbonation reaction, N is the cycle number, and f = 0.782 and b = 0.174 are constants obtained from a curve fit of several experimental studies by other researchers. The results of this curve fit compared to experimental data are shown in Fig. 7. A wide variety of synthetic sorbents designed to reduce degradation over multiple cycles have been studied recently, including calcium aluminate supported CaO (Manovic and Anthony,

Table 1. Summary of rate equations for calcination.

Rate equation	Rate Constant	Ref.
$\ln(1-X) = -k_s a t$	$k_s = 2.5 \times 10^{-8}$ mol/cm^2/s	Borgwardt (1985)
$r_c = \bar{k}(p^*_{CO_2} - p_{CO_2})$	$\bar{k}$ = 0.207 mol/bar/m^2/s	Dennis and Hayhurst (1987)
$\frac{dX}{dt} = k\frac{(1-X)(p_{eq}-p_{CO_2})}{p_{eq}}$, $k = k_0 \exp(\frac{-E_a}{RT})$	$k_0 = 2.12 \times 10^6 - 4.82 \times 10^{10}$ s^{-1}, E_a = 180.56–257.78 kJ/mol, dependent on atmosphere	Acharya *et al.* (2012)
$\frac{dX}{dt} = k(1-X)^m$, $k = k_0 \exp(\frac{-E_a}{RT})$	$k_0 = 6.45 \times 10^5$ s^{-1}, E_a = 187.3 kJ/mol	Gallagher and Johnson (1973)

Table 2. Summary of rate equations for carbonation.

Rate equation	Rate Constant	Ref.
$\frac{dX}{dt} = kCX_{max}\exp(-kCt)$	k = 25 m^3/mol/s	Shimizu *et al.* (1999)
$\frac{1}{\psi}[\sqrt{1-\psi\ln(1-X)}-1] = \frac{k_s a_0 (C-C_{eq})t}{2(1-\varepsilon_o)}$, $\frac{1}{\psi}[\sqrt{1-\psi\ln(1-X)}-1] = \frac{a_0}{(1-\varepsilon_o)}\sqrt{\frac{bMC_s t}{2c\rho Z}}$	k_s=0.0595 cm^4/mol/s	Bhatia and Perlmutter (1983)
$\frac{dX}{dt} = k_c(1-\frac{X}{X_{max}})^m(C_{CO_2}-C_{eq,CO_2})$	Kinetically controlled: k_c = 0.0021 m^3 mol/s, m = 2/3 Diffusion controlled: k_c = 0.0025 m^3 mol/s, m = 4/3	Fang *et al.* (2009)

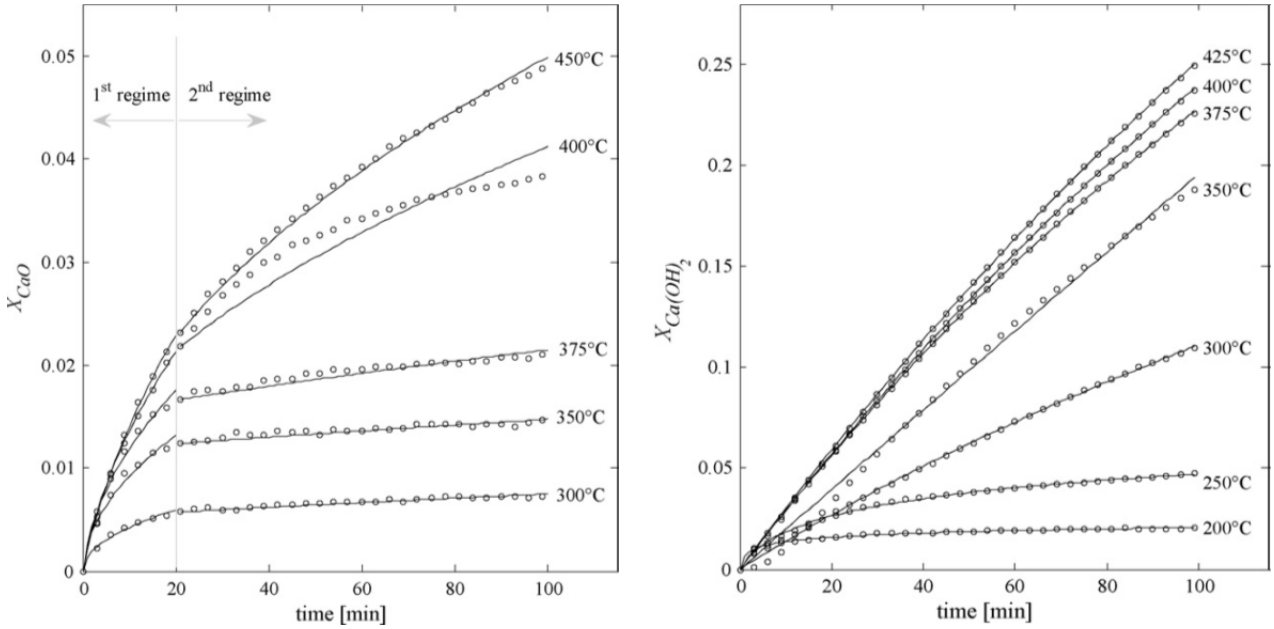

Fig. 6. Carbonation reaction extent as a function of time for CaO (a) and $Ca(OH)_2$ (b). Data points indicate experimental measurements and solid lines indicate numerical modeling results (Nikulshina *et al.*, 2007). Reproduced with permission from Elsevier.

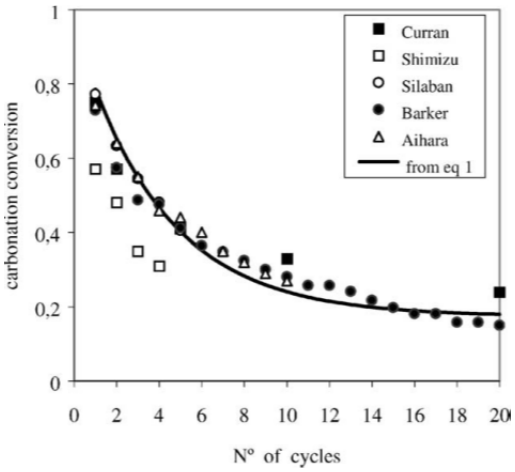

Fig. 7. Degradation of carbonation conversion with increasing number of cycles. Solid line calculated from Eq. (4) (Abanades, 2002). Reproduced with permission from Elsevier.

2009), CaO with a mayenite ($Ca_{12}Al_{14}O_{33}$) binder (Li *et al.*, 2006), CuO/CaO composite (Manovic *et al.*, 2011), CaO calcined from mesoporous $CaCO_3$ (Iyer *et al.*, 2004), thermal pretreatment of CaO (Can Ozcan *et al.*, 2011), and CaO prepared with various precursors (Lu *et al.*, 2006).

This summary of the kinetic analyses demonstrates that the kinetics of the calcination and carbonation reactions vary widely depending on the sorbent source and gas atmosphere composition. Overcoming the degradation of the sorbent is an important challenge addressed by on-going research in the field. A careful choice of sorbent is necessary to ensure fast reactions and an economical process without a need for frequent sorbent replacement.

HEAT AND MASS TRANSFER ANALYSES

In addition to chemical kinetics, interparticle physical processes of interest include mass transfer of gaseous reactants through the pore network, heat transfer to the endothermic reactions or from the exothermic reactions, and changing particle morphology. Global reaction rates and total particle conversion are influenced by local chemical kinetics, local reactant concentration, and local total pressure and temperatures. Numerical models have been developed to investigate mass and heat transfer limitations on reaction rates and total reaction extent at the particle level.

Calcination Modeling

Mass transfer in particles undergoing calcination has been investigated by Silcox *et al.* (1989) and García-Labiano *et al.* (2002). Diffusion through particle pores is the predominant mode of mass transfer in particles undergoing calcination. The local, transient concentration of carbon dioxide was predicted using the following one-dimensional (1D) conservation equation:

$$\frac{1}{r^2}\frac{\partial}{\partial r}\left(D_e r^2 \frac{\partial \psi_{CO_2}}{\partial r}\right) + \dot{S}_{\psi} = \frac{\partial \psi_{CO_2}}{\partial t} \tag{5}$$

Eq. (5) has been utilized in models with ψ representing partial pressure, concentration, or density. It has been employed in several analyses of both the calcination and carbonation reactions (Silcox *et al.*, 1989; García-Labiano *et al.*, 2002; Stendardo and Foscolo, 2009; Khoshandam *et al.*, 2010; Ebner and Lipiński, 2011, 2012; Yu *et al.*, 2012). The source term $\dot{S}_{\psi}$ was defined in terms of the chemical

reaction rates. Effective diffusivity of carbon dioxide in a porous media has been treated in the above models as a combination of bulk diffusivity and Knudson diffusivity and scaled by particle porosity. Boundary conditions were defined by spherical symmetry at the particle center (zero mass flux) and external mass transfer at the surface.

García-Labiano *et al.* (2002) investigated different rate expressions and determined kinetic parameters by fitting the changing grain size and shrinking core chemical reaction models to experimental data for the calcination of three different calcium based sorbents. They also investigated the effect of total pressure and postulated that total pressure influences the reaction rate because of its influence on effective gas diffusivity.

Models for investigating heat transfer by conduction and radiation within reacting particles have also been developed. Heat transfer properties related to conduction and radiation at the particle surface and within the particle volume vary greatly with temperature and the morphological changes in porosity and pore structure that accompany chemical reaction. A numerical model for investigating semi-transparent particles with spectral radiative properties in high-temperature applications was developed by Dombrovsky and Lipiński (2007). The model was applied to the transient heating of calcium carbonate and zinc oxide particles by concentrated solar radiation and predicts considerable temperature gradients within the particles as they are heated.

Lipiński and Steinfeld (2004a) first investigated a fixed bed of reacting particles. They numerically simulated the coupled radiative heat transfer and chemical reaction in a non-gray, non-isothermal, fixed bed of $CaCO_3$ particles undergoing calcination and found good agreement between model results and experimental data. The unsteady energy equation was solved inside the fixed bed by finite volume techniques. The incident solar radiation distribution was established with the Monte Carlo ray-tracing method. The radiative heat transfer through the bed was modeled with the Rosseland diffusion approximation. A contracting geometry rate law with an Arrhenius temperature dependence of the rate constant was employed. The heat transfer model was validated via comparison of computed and experimentally measured variations of temperatures and reaction extents.

Lipiński and Steinfeld (2004b) investigated a slab of suspended, reacting particles. They used a similar formulation for chemical kinetics as Lipiński and Steinfeld (2004a) to numerically simulate radiative heat transfer and chemical reaction in an absorbing, emitting, and Mie-scattering suspension of $CaCO_3$ particles undergoing calcination. They considered both shrinking and non-shrinking particles and showed radiation absorption was less efficient for shrinking particles. As a result of the less efficient absorption, the shrinking particle reaction rate was slower than the non-shrinking particle reaction rate. In the shrinking particle case, radiative properties varied as particle size changed and the absorption coefficient, scattering coefficient, and scattering phase function had to be calculated at each time step.

A transient model incorporating heat transfer, mass transfer, and chemical kinetics has been analyzed by Ebner and Lipiński (2011) (Fig. 8). Eq. (5) was solved along with the energy conservation equation formulated as

$$\overline{\overline{\rho c_p}} \frac{\partial T}{\partial t} = -\nabla \cdot \vec{\mathbf{q}} + \dot{S}_{\text{chem}} \tag{6}$$

Two methods for modeling radiative heat transfer were considered: Rosseland diffusion approximation and Monte Carlo ray tracing method. Ebner and Lipiński (2011) found that including radiation significantly increased the rate of particle heating and subsequently decreased the time to complete particle calcination. Temperatures predicted by the Rosseland diffusion approximation were in good agreement with those predicted by the Monte Carlo ray tracing method. The effect of the grain size of calcium oxide strongly influence the optical behavior of the particle, but was investigated and found to only weakly influence temperature, reaction extent, and total reaction time.

Ebner and Lipiński (2012) used the same formulation for heat and mass transfer to investigate two methods for modeling the calcination rate and resulting particle: changing grain size model and shrinking core model. The two approaches were compared and conditions under which the reaction was heat transfer limited or mass transfer limited were identified.

Carbonation Modeling

Mass transfer in particles undergoing carbonation has been approached in a similar manner as in particles undergoing calcination. Stendardo and Foscolo (2009) and Khoshandam *et al.* (2010) developed models coupling mass transfer and carbonation chemical kinetics. In carbonating particles, as the product layer of calcium carbonate develops, pores shrink and a large fraction of them eventually close, a product layer shell is formed, and mass transfer is restricted. As pore diffusion is impeded, diffusion through the product layer of calcium carbonate becomes a significant

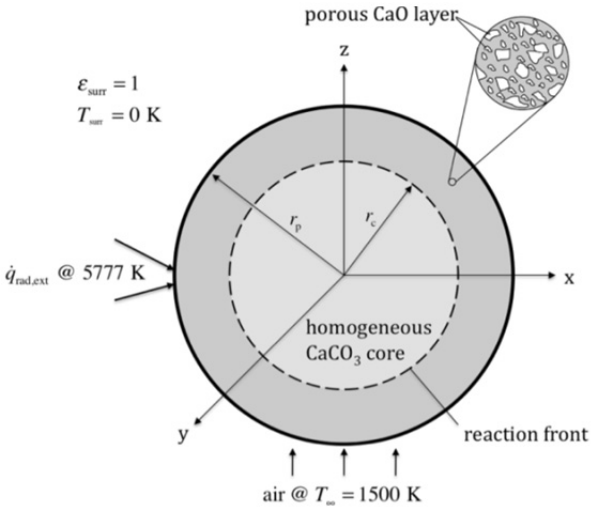

Fig. 8. Semitransparent particle undergoing heterogeneous decomposition under high flux irradiation (Ebner and Lipinski, 2011). Reproduced with permission from Elsevier.

factor. Both phenomena were carefully considered in the model developed by Stendardo and Foscolo (2009). They were able to predict total reaction extent for cases in which complete conversion could not be experimentally reached due to mass transfer limitations through the developed product layer.

A complete model solving equations for conservation of mass, Eq. (5), conservation of energy, Eq. (6) with $\vec{\mathbf{q}}$ limited to conduction, and chemical kinetics for carbonation was numerically analyzed for a particular type of sorbent particle by Yu *et al.* (2012). They did not consider pure or relatively pure calcium oxide sorbent samples but analyzed a special sorbent particle made of very small calcium oxide particles suspended in a porous spherical supporting material. Good correlation was observed between the model and experimental data.

SOLAR REACTOR ENGINEERING

Early experimental work has focused on the calcination of $CaCO_3$ for the solar production of lime as a commodity or as an energy storage material. Several reactor types have been used for this process, including fluidized bed (Badie *et al.*, 1980; Flamant *et al.*, 1980), rotary kiln (Badie *et al.*, 1980; Flamant *et al.*, 1980; Meier *et al.*, 2003; Meier *et al.*, 2004; Meier and Cella, 2004; Meier *et al.*, 2005; Meier *et al.*, 2006), and cyclone or vortex flow reactors (Imhof *et al.*, 1991; Nikulshina *et al.*, 2009a; Steinfeld *et al.*, 1992). $CaCO_3$ was fed to the reactors in the form of particles with sizes ranging from a few μm to a few mm. The reactors were subjected to 1–5 kW of concentrated solar radiation input, provided by a solar furnace, consisting of a sun-tracking heliostat and a stationary parabolic concentrator, or by a high-flux solar simulator, consisting of high-pressure Ar arc lamps close-coupled to elliptical reflectors. Experimentally measured quantities include temperatures, measured with thermocouples or with a pyrometer, reaction extents, determined via X-ray diffraction or by complete calcination of product samples in a TG, and radiative power input to the reactor, determined from calibrated gray-scale images of a Lambertian (diffusely reflecting) target at the focus of the concentrating system.

Flamant *et al.* (1980) and Badie *et al.* (1980) conducted the calcination of $CaCO_3$ particles in fluidized bed and rotary kiln reactors (Fig. 9). The fluidized bed reactor was comprised of a vertical silica tube (5) with a gas distributor (3) consisting of inert (metallic or ceramic; 0.6–0.8 mm-dia.) beads lying on a metallic grid. The lower part of the tube was surrounded by a cylindrical reflector (9) to reduce reflection and reradiation losses. The solar absorption and consequently the solar energy conversion efficiency of the reactor was enhanced by doping the $CaCO_3$ particles with 1 weight-% of graphite. Complete decomposition of a batch of 10 g of particles was accomplished after 6–8 min of operation at around 850°C bulk temperature, resulting in an energy conversion efficiency (ratio of sensible energy plus reaction enthalpy to incident solar energy) of 10–15%. The rotary kiln consisted of a rotating water-cooled cylindrical metallic shell (7), with its inner wall lined with a refractive

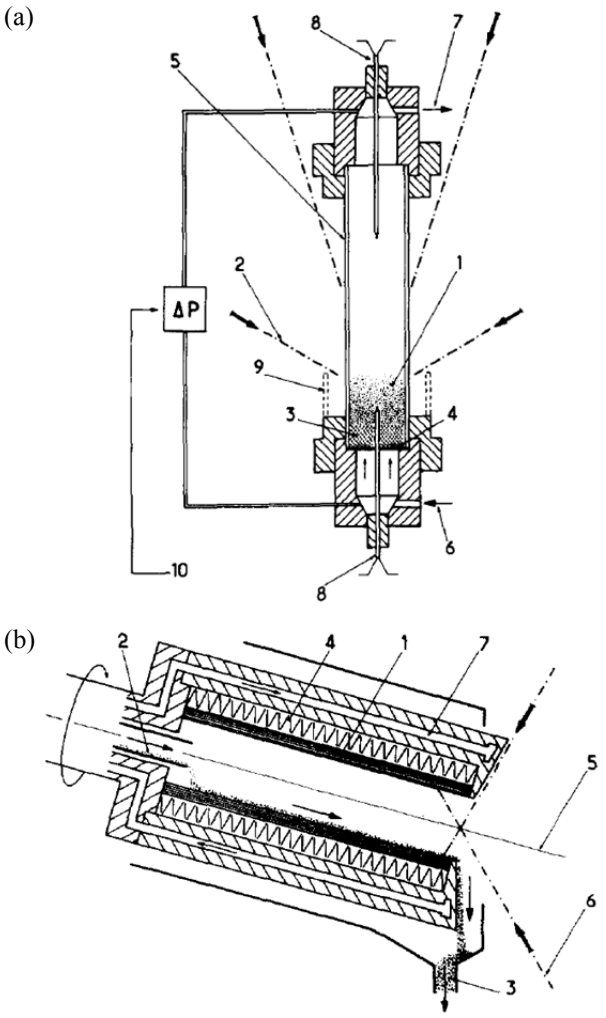

Fig. 9. Fluidized bed and rotary kiln reactors tested by (Badie *et al.*, 1980). Reproduced with permission from Elsevier.

tube (1) (alumina or lanthanum chromite). Particles were fed through a vibrating tube in the back of the reactor (2) and were transported to the front due to the rotation of the 5° inclined cavity. For the rotary kiln reactor in continuous operation, optimum efficiency of 7% was achieved at 30% conversion with a feed rate of 0.077 g/s and a rotation speed of 8 rpm; the highest reported conversion was 50%. While nearly uniform temperature distribution was measured over a large portion of the fluidized bed, temperature variations of more than 1000°C were observed in the rotary kiln.

Salman and Khraishi (1988) partially calcined a $CaCO_3$ pellet contained in a graphite tube, surrounded by a stainless steel box with a windowed opening. Conversions ranging from 17% at 1165°C to 65% at 1446°C were measured. Non-uniform heating of the pellet was identified to be the reason for the lower reaction rates as compared with experiments conducted in electric furnaces, and the use of a fluidized bed reactor was suggested to improve the heat and mass transfer.

Imhof (1991), Imhof *et al.* (1991) and Steinfeld *et al.* (1992) developed and tested cyclone reactors. The cyclone reactor tested by Steinfeld *et al.* (1992) consisted of a 30 cm-long truncated steel cone (10° opening angle), insulated

with 12 cm-thick alumina-silica insulation. Two concentric conical plates with a 6-cm open aperture covered the larger end section of the cone. A tangential air flow with suspended $CaCO_3$ particles entered the reactor beneath the lower conical cover plate. Due to the swirl of the flow, the particles separated from the flow at the wall and exited through the smaller end section of the cone. The reactor was operated at 1200–1450 K wall temperature, and degrees of particle conversion in the range 53 to 100% were measured.

Meier *et al.* (2003, 2004), Meier and Cella (2004) and Meier *et al.* (2005a, b, 2006) developed and tested 10 kW rotary kiln reactors for the calcination of 1–5 mm large $CaCO_3$ particles. Meier *et al.* (2004) developed a horizontal cylindrical cavity reactor, consisting of a conical reaction chamber, made from refractory concrete. The reactor was insulated with fibrous ceramic material encapsulated in a stainless steel shell. The entire reactor sat on four rubber wheels which were driven by an electric motor to rotate the cavity. Solar radiation entered through a 8 cm-dia. circular aperture in the reactor's water cooled aluminum front. The $CaCO_3$ particles (98% purity) were fed from a hopper to the back of the reactor. Due to the rotation of the conical reaction chamber, the particles were transported through the reactor, where they were directly exposed to solar radiation. The calcined particles were collected in a bin below the reactor front. The reactor was tested on sun for a total of 100 h. Tests were run for 30 min at steady-state with a constant particle flow rate. Degrees of calcination > 98% and efficiencies up to 20% were determined experimentally. The efficiency was defined as the ratio of the enthalpy of the produced CaO to the solar power input to the reactor:

$$\eta = \frac{\dot{m}_{CaO}\Delta H^{o}_{298K}}{\dot{Q}_{solar}} \tag{7}$$

For a typical test run with η = 13%, energy losses were due to natural convection from the open aperture and losses via unrecovered products (50% of the solar power input), reradiation losses (17%), sensible heat of products (10%), and conduction through insulation (10%).

Meier *et al.* (2003, 2005b, 2006) developed an indirectly heated rotary kiln reactor, consisting of 16 SiC absorber tubes, which were contained in a tilted rotating cylindrical solar cavity with a circular aperture (Fig. 10). 1–5 mm large limestone particles were fed from the back of the reactor through a preheating chamber into the tubes, and the products were collected with a funnel at the front of the cavity. Experimentally determined efficiencies, calculated according to Eq. (7), reached 32%. The energy balance of the reactor accounted for the solar power input to the reactor, the heat rate to heat the reactants, the energy input to the dissociation reaction of $CaCO_3$, reradiation and conduction heat losses, a lumped heat loss term that accounted for unknown heat losses such as convection heat losses through the aperture and heat losses via unrecovered products, and the heat stored in the reactor during transients:

$$\dot{Q}_{solar} - (\dot{Q}_{heating} + \dot{Q}_{diss} + \dot{Q}_{reradiation} + \dot{Q}_{conduction} + \dot{Q}_{other} + \dot{Q}_{storage}) = 0 \tag{8}$$

The relative magnitude of the energy balance terms are shown in Fig. 11 for experiments with various parameter settings. The design and principal dimensions of scale-up reactors with solar power input of 0.5 to 20 MW were described.

A 10-kW_{th} solar-heated rotary kiln for multiple applications in solar thermochemical processing was developed, tested and modeled at the German Aerospace Center (DLR) (Neises *et al.*, 2012; Tescari *et al.*, 2013). While it was experimentally demonstrated for thermal reduction of

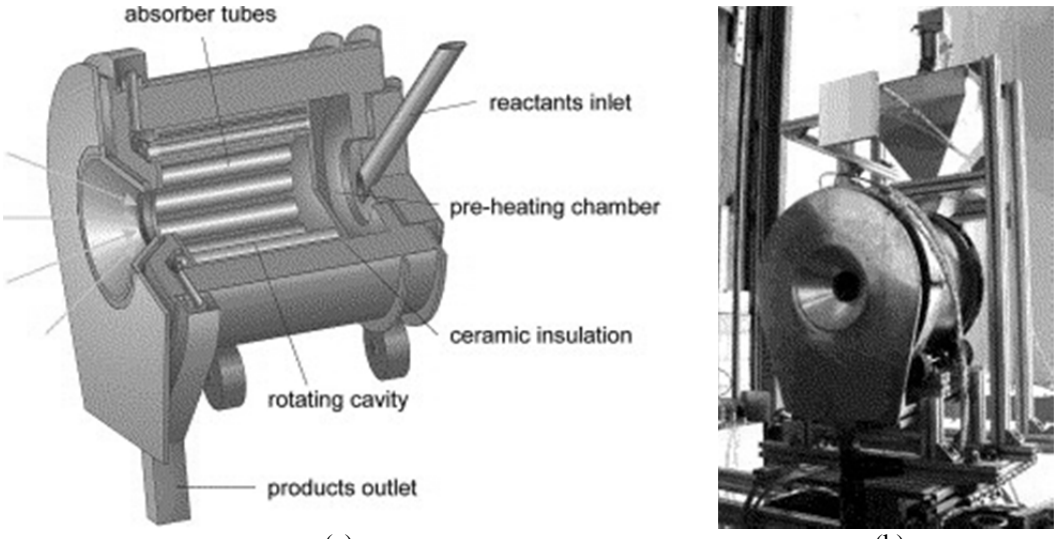

(a) (b)

Fig. 10. Schematic (a) and photograph (b) of a rotary kiln reactor consisting of 16 SiC absorber tubes (250 mm-length, 17 mm-i.d.) contained in a 250 mm-i.d. SiC cavity with 76 mm-thick dual-layer ceramic insulation, and a 2 mm thick steel drum (Meier *et al.*, 2006). Reproduced with permission from Elsevier.

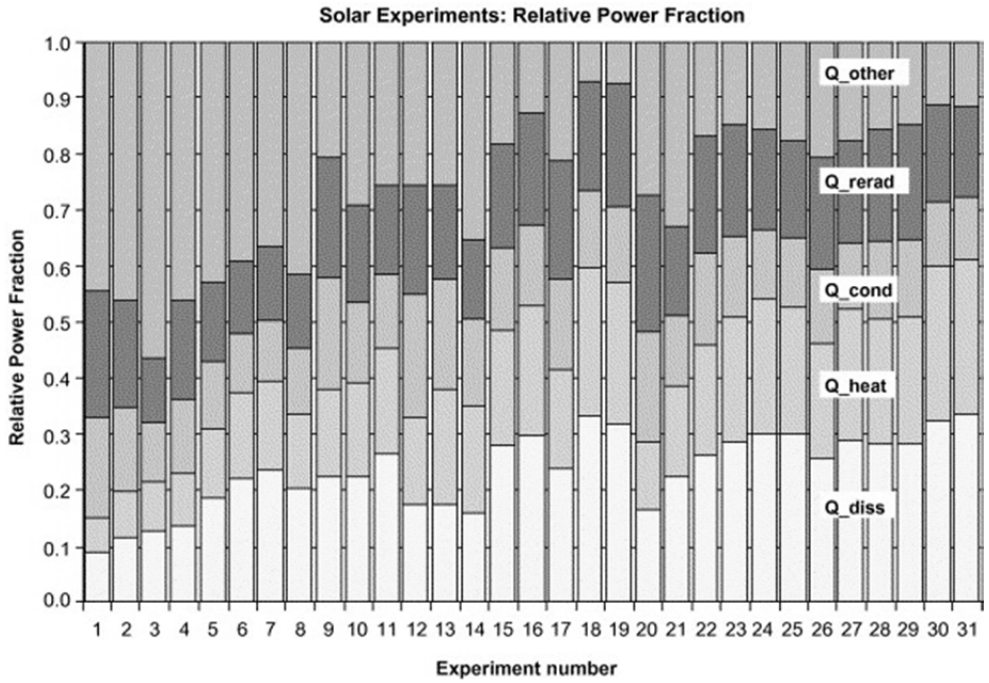

Fig. 11. Energy balance terms, Eq. (8), normalized by the net solar power input, $\dot{Q}_{solar} - \dot{Q}_{storage}$, for on-sun experiments with various parameter settings: rotational speed (8–18 rpm), particle feed rate (36–136 g/min), limestone grain size (2–3 mm), and temperature (1200–1400 K) (Meier *et al.*, 2006). Reproduced with permission from Elsevier.

metal oxides for thermochemical energy storage, this reactor concept, due to the possibility of implementing a moving particle bed in a rotary kiln, can be considered for solar-driven calcination of limestone particles.

Nikulshina *et al.* (2009b) conducted 5 consecutive carbonation-calcination cycles in a fluidized-bed solar reactor (Fig. 12). The reactor consisted of a silica tube (22 mm i.d., 260 mm length) containing 7 g of a mixture of 97 wt% inert silica particles (229 µm mean particle size) and 3 wt% CaO particles (9µm mean particle size), directly exposed to concentrated solar radiation. Carbonation was conducted during 600 s at 365–400°C in a flow of 2 L(STP)/min of synthetic air containing 500 ppm of CO_2 and 17% water vapor. Calcination was conducted during approx. 600 s at 800–875°C in an Ar-flow of 1.75 L(STP)/min. The CO_2 evolution during the 5 cycles shown in Fig. 13 demonstrated that completely CO_2-depleted air exited the reactor during the carbonation steps and that the calcination reaction reached completion after around 500 s. Sorbent deactivation was not observed after 5 cycles, which was attributed to the addition of steam during carbonation, and to the relatively low calcination temperature. A reduction of the particle size from 9 to 1.5 µm and consequently an increase of the BET surface area were observed, which was explained by the cracking of the particles due to the $Ca(OH)_2$ formation inside the particles. Single long-term (4000 s) carbonation experiments yielded higher reaction extent with CaO than with $Ca(OH)_2$ particles (71 vs. 61%).

The coproduction of syngas and lime by combined calcination of $CaCO_3$ particles and dry-reforming of methane in a 5 kW vortex flow reactor has been experimentally demonstrated by Nikulshina *et al.* (2009a). A flow of CH_4, diluted in Ar and laden with $CaCO_3$ particles was injected behind the aperture of a cylindrical cavity reactor and exited through an opening in the back wall. Methane conversion ($X_{CH_4} = 1 - n_{CH_4,out}/n_{CH_4,in}$) was determined via measured inlet and outlet flow rates and gas compositions; $CaCO_3$ conversions ($X_{CaCO_3} = n_{CaO}/(n_{CaO_3} + n_{CaO})$ was determined from TG measurements during the complete calcination of solid product samples. Highest CH_4 and $CaCO_3$ conversions were $X_{CH_4} = 0.38$ and $X_{CaCO_3} = 0.83$, respectively, at a reactor temperature of 1223 K, and the energy conversion efficiency was 7–10%.

SUMMARY

Carbon dioxide is an important commodity in multiple state-of-the-art industries. The demand for pure CO_2 may substantially increase in mid- to long-term as it is considered, beside water, as an input for solar-driven hydrocarbon fuel production. Carbon dioxide capture technologies are one option to provide carbon dioxide for these applications which simultaneously address the challenge of climate change mitigation. Carbon dioxide capture methods can be divided into the categories of absorption, adsorption, membrane separation, and cryogenic separation. One absorption method that has been investigated is the CaO-based carbonation-calcination cycle. Thermodynamic analyses have shown that the cycle is well suited to separation applications with high CO_2 concentrations, such as power plant flue gases. Heat recovery will play an important role in reducing the energy required for the process. Kinetic analyses have shown that the calcination reaction is relatively fast, but the carbonation reaction speed is limited by the switch to a

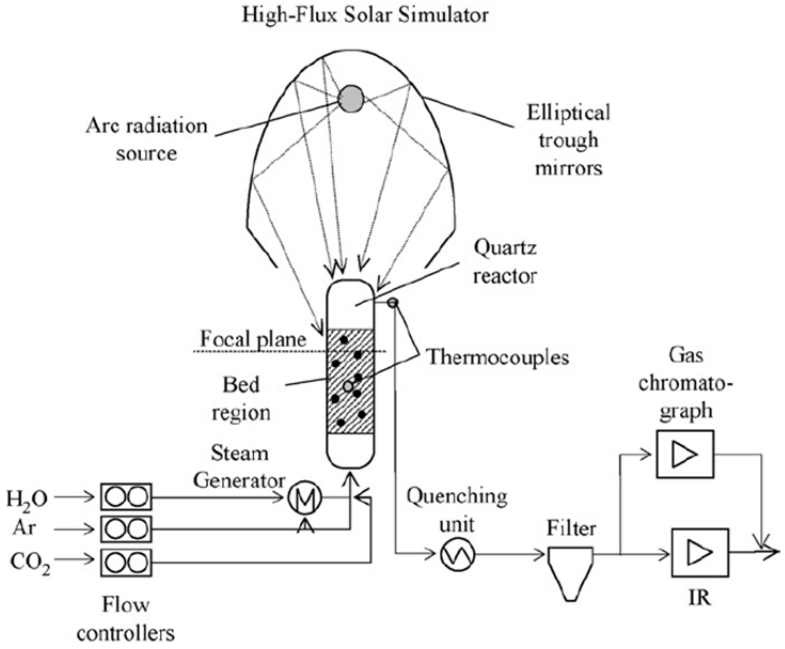

Fig. 12. Schematic of the fluidized bed solar reactor setup tested by (Nikulshina *et al.*, 2009) and (Nikulshina and Steinfeld, 2009). Reproduced with permission from Elsevier.

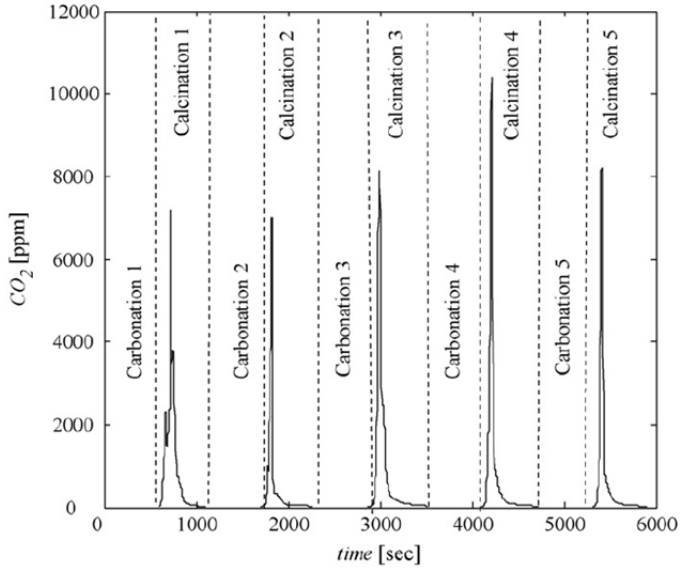

Fig. 13. CO_2 evolution during carbonation-calcination cycling (Nikulshina *et al*., 2009). Reproduced with permission from Elsevier.

diffusion controlled regime due to the formation of a $CaCO_3$ product layer on the outside of the particles. Sorbent degradation over multiple cycles is also a known problem, but many potential solutions have been proposed for reducing it. Heat and mass transfer modeling at the particle level has shown good agreement with experimental data. Several solar reactors with input power of up to 10 kW to accomplish the calcination step of the process have been investigated, reaching efficiencies of up to 32%. Advancements towards more efficient and cost effective solar-driven CO_2 capture via thermochemical looping include development of new sorbents that resist degradation and development of solar reactors that accomplish the full cycle at high efficiencies and CO_2 capture rates.

ACKNOWLEDGEMENTS

The financial support by the University of Minnesota Initiative for Renewable Energy and the Environment (grant no. RC-0009-12) is gratefully acknowledged. Leanne Reich has been supported by the National Science Foundation Graduate Research Fellowship (grant no. 00006595).

NOMENCLATURE

a	molar specific surface area, cm^2/mol
a_0	initial surface area per unit volume, m^{-1}
b, c	stoichiometric coefficients
b	constant in Eq. (4)
$\underline{C}$	molar concentration, mol/m^3
$\underline{c}_p$	molar heat capacity at constant pressure, J/mol/K
D	diffusivity, m^2/s
E_a	activation energy, kJ/mol
f	constant in Eq. (4)
$\Delta\underline{h}^o_{298K}$	standard molar enthalpy of reaction, kJ/mol
k	reaction rate constant, various units
L_0	initial pore system length per unit volume, m^{-2}
$\dot{m}$	mass flow rate, kg/s
n	amount of substance, mol
N	number of cycles
p	pressure, Pa
$\dot{q}$	heat flux, W/m^2
$\dot{Q}$	heat rate, W
$\underline{Q}$	heat per amount of substance, kJ/mol
r	radial coordinate, m
r_c	rate of calcination, $kmol/m^2/s$
R	universal gas constant, $R = 8.31$ J/mol/K
$\dot{S}$	heat or mass source term, various units
t	time, s
$\underline{T}$	temperature, K
$\underline{x}$	molar fraction
X	reaction extent
X_{max}	maximum reaction conversion
Z	ratio of volume in solid phase after reaction to that before reaction

Greek

ε_o	initial porosity
$\underline{\eta}$	efficiency
$\underline{\rho}$	molar density, mol/m^3
ψ	general variable in Eq. (5), various units; structural parameter, $\psi = \frac{4\pi L_o(1-\varepsilon_o)}{a_0^2}$

Subscripts

chem	heat source due to chemistry
CO_2	carbon dioxide
eq	equilibrium
H_2O	water
0	initial
1…9	at positions indicated in Fig. 4
φ	mass source due to chemistry

REFERENCES

Aaron, D. and Tsouris, C. (2005). Separation of CO_2 from Flue Gas: A Review. *Sep. Sci. Technol.* 40: 321–348.

Abanades, J.C. (2002). The Maximum Capture Efficiency of CO_2 Using a Carbonation/Calcination Cycle of $CaO/CaCO_3$. *Chem. Eng. J.* 90:303–306.

Abanades, J.C., Rubin, E.S. and Anthony, E.J. (2004a). Sorbent Cost and Performance in CO_2 Capture Systems. *Ind. Eng. Chem. Res.* 43: 3462–3466.

Abanades, J.C., Anthony, E.J., Lu, D.Y., Salvador, C. and Alvarez, D. (2004b). Capture of CO_2 from Combustion Gases in a Fluidized Bed of CaO. *AlChE J.* 50: 1614–1622.

Acharya, B., Dutta, A. and Basu, P. (2012). Circulating-fluidized-bed-based Calcium-looping Gasifier: Experimental Studies on the Calcination-carbonation Cycle. *Ind. Eng. Chem. Res.* 51: 8652–8660.

Badie, J.M., Bonet, C., Faure, M. and Flamant, G. (1980). Decarbonation of Calcite and Phosphate Rock in Solar Chemical Reactors. *Chem. Eng. Sci.* 35: 413–420.

Bhatia, S.K. and Perlmutter, D.D. (1983). Effect of the Product Layer on the Kinetics of the CO_2-lime Reaction. *AlChE J.* 29: 79–86.

Borgwardt, R.H. (1985). Calcination Kinetics and Surface Area of Dispersed Limestone Particles. *AlChE J.* 31: 103–111.

BP Statistical Review of World Energy (2012). http://www.bp.com/liveassets/bp_internet/globalbp/globalbp_uk_english/reports_and_publications/statistical_energy_review_2011/STAGING/local_assets/pdf/statistical_review_of_world_energy_full_report_2012.pdf (Accessed July 5, 2012).

Can Ozcan, D., Shanks, B.H. and Wheelock, T.D. (2011). Improving the Stability of a CaO-based Sorbent for CO_2 by Thermal Pretreatment. *Ind. Eng. Chem. Res.* 50: 6933–6942.

Chapel, D., Ernest, J. and Mariz, C. (1999). Recovery of CO_2 from Flue Gases: Commercial Trends, Canadian Society of Chemical Engineers Annual Meeting, Saskatoon, Saskatchewan, Canada.

Chueh, W., Falter, C., Abbott, M., Scipio, D., Furler, P., Haile, S.M. and Steinfeld, A. (2010). High-flux Solar Driven Thermochemical Dissociation of CO_2 and H_2O Using Nonstoichiometric Ceria. *Science* 330: 1797–1801.

Dennis, J.S. and Hayhurst, A.N. (1987). The effect of CO_2 on the Kinetics and Extent of Calcination of Limestone and Dolomite Particles in Fluidized Beds. *Chem. Eng. Sci.* 42: 2361–2372.

Dombrovsky, L. and Lipiński, W. (2007). Transient Temperature and Thermal Stress Profiles in Semi-transparent Particles under High-flux Irradiation. *Int. J. Heat Mass Transfer* 50: 2117–2123.

Ebner, P.P. and Lipiński, W. (2011). Heterogeneous Thermochemical Decomposition of a Semi-transparent Particle under Direct Irradiation. *Chem. Eng. Sci.* 66: 2677–2689.

Ebner, P.P. and Lipiński, W. (2012). Heterogeneous Thermochemical Decomposition of a Semi-transparent Particle under High-flux Irradiation—Changing Grain Size vs. Shrinking Core Models. *Numer. Heat Transfer, Part A* 62: 412–431.

Escardino, A., Garcia-Ten, J. and Feliu, C. (2008). Kinetic Study of Calcite Particle (Powder) Thermal Decomposition: Part I. *J. Eur. Ceram. Soc.* 28: 3011–3020.

Fang, F., Li, Z. and Cai, N. (2009). Experiment and Modeling of CO_2 Capture from Flue Gases at High

Temperature in a Fluidized Bed Reactor with Ca-based Sorbents. *Energy Fuels* 23: 207–216.

Flamant, G., Hernandez, D., Bonet, C. and Traverse, J. (1980). Experimental Aspects of the Thermochemical Conversion of Solar Energy Decarbonation of $CaCO_3$. *Sol. Energy* 24: 385–395.

Fletcher, E.A. (2001). Solarthermal Processing: A Review. *J. Sol. Energy Eng.* 123: 63–74.

Gallagher, P.K. and Johnson, D.W. (1973). The Effects of Sample Size and Heating Rate on the Kinetics of the Thermal Decomposition of $CaCO_3$. *Thermochim. Acta* 6: 67–83.

Garcia-Labiano, F., Abad, A., de Diego, L.F., Gayan, P. and Adanez, J. (2002). Calcination of Calcium-based Sorbents at Pressure in a Broad Range of CO_2 Concentrations. *Chem. Eng. Sci.* 57: 2381–2393.

Gupta, H. and Fan, L.S. (2002). Carbonation-calcination Cycle Using High-reactivity Calcium Oxide for Carbon Dioxide Separation from Flue Gas. *Ind. Eng. Chem. Res.* 41: 4035–4042.

Hathaway, B.J., Davidson, J.H. and Kittelson, D.B. (2011). Solar Gasification of Biomass: Kinetics of Pyrolysis and Steam Gasification in Molten Salt. *J. Sol. Energy Eng.* 133: 021011.

IEA Greenhouse Gas R&D Programme (1994). *Carbon Dioxide Capture from Power Stations*, London.

Imhof, A. (1991). The Cyclone Reactor – An Atmospheric Open Solar Reactor. *Sol. Energy Mater.* 24: 733–741.

Imhof, A., Suter, C. and Steinfeld, A. (1991). Solar Thermal Decomposition of $CaCO_3$ on an Atmospheric Open Cyclone Reactor. In *1991 Solar World Congress*, Arden, M.E., Burley, S.M.A., and Coleman, M. (Eds.), Proceedings of the Biennial Congress of the International Solar Energy Society, Denver, Colorado, USA, 1991, Permagon Press, p. 2091–2096.

Iyer, M.V., Gupta, H., Sakadijan, B.B. and Fan, L.S. (2004). Multicyclic Study on the Simultaneous Carbonation and Sulfation of High-reactivity CaO. *Ind. Eng. Chem. Res.* 43: 3939–3947.

Kalafati, D.D. (1991). Diffusion Entropy and Theoretical Separative Work for Gas Mixtures with Variable Concentration. *Inzh. Fiz. Zh.* 61: 598–604.

Khoshandam, B., Kumar, R.V. and Allahgholi, L. (2010). Mathematical Modeling of CO_2 Removal Using Carbonation with CaO: The Grain Model. *Korean J. Chem. Eng.* 27: 766–776.

Kodama, T. and Gokon, N. (2007). Thermochemical Cycles for High-temperature Solar Hydrogen Production. *Chem. Rev.* 107: 4048–4077.

Leckel, D. (2009). Diesel Production from Fischer-Tropsch: The Past, the Spresent, and New Concepts. *Energy Fuels* 23: 2342–2358.

Li, Z., Cai, N. and Huang, Y. (2006). Effect of Preparation Temperature on Cyclic CO_2 Capture and Multiple Carbonation-calcination Cycles for a New Ca-based CO_2 Sorbent. *Ind. Eng. Chem. Res.* 45: 1911–1917.

Lipinski, W. and Steinfeld, A. (2004a). Heterogeneous Thermochemical Decomposition under Direct Irradiation. *Int. J. Heat Mass Transfer* 47: 1907–1916.

Lipiński, W. and Steinfeld, A. (2004b). Transient Radiative Heat Transfer within a Particle Suspension Undergoing Endothermal Decomposition—Shrinking vs. Non-shrinking Particles. *ICHMT Digital Library Online* 16, doi: 10.1615/ICHMT.2004.RAD-4.300.

Lu, D.Y., Hughes, R.W. and Anthony, E.J. (2008). Ca-based Sorbent Looping Combustion for CO_2 Capture in Pilot-scale Dual Fluidized Beds. *Fuel Process. Technol.* 89: 1386–1395.

Lu, H., Reddy, E.P. and Smirniotis, P.G. (2006). Calcium Oxide Based Sorbents for Capture of Carbon Dioxide at High Temperatures. *Ind. Eng. Chem. Res.* 45: 3944–3949.

Manovic, V. and Anthony, E.J. (2009). CaO-based Pellets Supported by Calcium Aluminate Cements for High-temperature CO_2 Capture. *Environ. Sci. Technol.* 43: 7117–7122.

Manovic, V., Wu, Y., He, I. and Anthony, E.J. (2011). Core-in-shell CaO/CuO-based Composite for CO_2 Capture. *Ind. Eng. Chem. Res.* 50:12384–12391.

Martinez, A., Lara, Y., Lisbona, P. and Romero, L.M. (2012). Energy Penalty Reduction in the Calcium Looping Cycle. *Int. J. Greenhouse Gas Control* 7:74–81.

Matthews, L. and Lipiński, W. (2012). Thermodynamic Analysis of Solar Thermochemical CO_2 Capture via Carbonation/Calcination Cycle with Heat Recovery. *Energy* 45: 900–907.

Meier, A., Wuillemin, D., Lipinski, W., Cella, G.M. and Bonaldi, E. (2003). European Patent Application 1-475-581-A1.

Meier, A. and Cella, G.M. (2004). Harnessing the Power of the Sun. *World Cem.* 35:25–35.

Meier, A., Bonaldi, E., Cella, G.M., Lipinski, W., Wuillemin, D. and Palumbo, R. (2004). Design and Experimental Investigation of a Horizontal Rotary Reactor for the Solar Thermal Production of lime. *Energy* 29: 811–821.

Meier, A., Gremaud, N. and Steinfeld, A. (2005a). Economic Evaluation of the Industrial Solar Production of Lime. *Energy Convers. Manage.* 46: 905–926.

Meier, A., Bonaldi, E., Cella, G.M. and Lipinski, W. (2005b). Multitube Rotary Kiln for the Industrial Solar Production of Lime. *J. Sol. Energy Eng.* 127: 386–395.

Meier, A., Bonaldi, E., Cella, G.M., Lipinski, W, and Wuillemin, D. (2006). Solar Chemical Reactor Technology for Industrial Production of Lime. *Sol. Energy* 80: 1355–1362.

Metz, B., Davidson, O., de Coninck, H.C., Loos, M., and Meyers, L.A. (2005). *IPCC Special Report on Carbon Dioxide Capture and Storage*, Cambridge University Press, Cambridge.

Neises, M., Tescari, S., de Oliveira, L., Roeb, M., Sattler, C. and Wong, B. (2012). Solar-heated Rotary Kiln for Thermochemical Energy Storage. *Sol. Energy* 86: 3040–3048.

Nikulshina, V., Hirsch, D., Mazzotti, M. and Steinfeld, A. (2006). CO_2 Capture from Air and Co-production of H_2 via the $Ca(OH)_2$–$CaCO_3$ Cycle Using Concentrated Solar Power—Thermodynamic Analysis. *Energy* 31: 1715–1725.

Nikulshina, V., Galvez, M.E. and Steinfeld, A. (2007).

Kinetic Analysis of the Carbonation Reactions for the Capture of CO_2 from Air via the $Ca(OH)_2$–$CaCO_3$–CaO Solar Thermochemical Cycle. *Chem. Eng. J.* 129: 75–83.

Nikulshina, V. and Steinfeld, A. (2009). CO_2 Capture from Air via CaO-carbonation Using a Solar Driven Fluidized Bed Reactor—Effect of Temperature and Water Vapor Concentration. *Chem. Eng. J.* 155: 867–873.

Nikulshina, V., Halmann, M. and Steinfeld, A. (2009a). Coproduction of Syngas and Lime by Combined $CaCO_3$-calcination and CH_4-reforming Using a Particle-Flow Reactor Driven by Concentrated Solar Radiation. *Energy Fuels* 23:6207–6212.

Nikulshina, V., Gebald, C. and Steinfeld, A. (2009b). CO_2 Capture from Atmospheric Air via Consecutive CaO-Carbonation and $CaCO_3$-calcination Cycles in a Fluidized-bed Solar Reactor. *Chem. Eng. J.* 146: 244–248.

Pierantozzi, R. (2003). Carbon Dioxide. *Kirk-Othmer Encyclopedia of Chemical Technology*, John Wiley and Sons, Inc.

Rackley, S.A. (2010). *Carbon Capture and Storage*, Butterworth-Heinemann/Elsevier, Burlington.

Rodriguez, N., Alonso, M., Grasa, G. and Abanades, J.C. (2008). Heat Requirements in a Calciner of $CaCO_3$ Integrated in a CO_2 Capture System Using CaO. *Chem. Eng. J.* 138: 148–154.

Rodriguez, N., Alonso, M., Abanades, J.C., Charitos, A., Hawthorne, C., Scheffknecht, G., Lu, D.Y. and Anthony, E.J. (2011). Comparison of Experimental Results from Three Dual Fluidized Bed Test Facilities Capturing CO_2 with CaO. *Energy Procedia* 4: 393–401.

Salman, O.A. and Khraishi, N. (1988). Thermal Decomposition of Limestone and Gypsum by Solar Energy. *Sol. Energy* 41: 305–308.

Shimizu, T., Hirama, T., Hosoda, H., Kitano, K., Inagaki, M. and Tejima, K. (1999). A Twin Fluid-bed Reactor for Removal of CO_2 from Combustion Processes. *Chem. Eng. Res. Des.* 77: 62–68.

Silcox, G.D., Kramlich, J. and Pershing, D.W. (1989). A Mathematical Model for the Flash Calcination of Dispersed $CaCO_3$ and $Ca(OH)_2$ Particles. *Ind. Eng. Chem. Res.* 28: 155–160.

Stalkup, F.I. (1978). Carbon Dioxide Miscible Flooding: Past, Present, and Outlook for the Future. *J. Pet. Technol.* 30: 1102–1112.

Steinfeld, A. and Palumbo, R. (2001). Solar Thermochemical Process Technology. In *Encyclopedia of Physical Science and Technology*, Vol. 15, Meyers, R.A. (Ed.), Academic Press, Burlington, p. 237.

Steinfeld, A., Imhof, A. and Mischler, D. (1992). Experimental Investigation of an Atmospheric-open cyclone Solar Reactor for Solid-gas Thermochemical Reactions. *J. Sol. Energy Eng.* 114: 171–174.

Steinfeld, A., Brack, M., Meier, A., Weidenkaff, A. and Wuillemin, D. (1998). A Solar Chemical Reactor for co-Production of Zinc and Synthesis Gas. *Energy* 23: 803–814.

Stendardo, S. and Foscolo, P.U. (2009). Carbon Dioxide Capture with Dolomite: A Model for Gas-solid Reaction within the Grains of a Particulate Sorbent. *Chem. Eng. Sci.* 64: 2343–2352.

Tescari, S., Neises, M., de Oliveira, L., Roeb, M., Sattler, C. and Neveu, P (2013). Thermal Model for the Optimization of a Solar Rotary Kiln to be Used as High Temperature Thermochemical Reactor. *Sol. Energy* 95: 279–289.

Tuinier, M.J., Hamers, H.P. and van Sint Annaland, M. (2011). Techno-economic Evaluation of Cryogenic CO_2 Capture—A Comparison with Absorption and Membrane Technology. *Control* 5: 1559–1565.

U.S. Energy Information Administration (2009). Emissions of Greenhouse Gases in the United States 2008, Technical Report for the Office of Integrated Analysis and Forecasting, U.S. Department of Energy, Washington, D.C.

U.S. Energy Information Administration (2011). International Energy Outlook 2011, Technical Report for the U.S. Department of Energy, Washington, D.C.

Wilson, E.J. and Gerard, D. (2007). *Carbon Capture and Sequestration: Integrating Technology, Monitoring, and Regulation*, Blackwell Pub., Ames.

Yu, Y.S., Liu, W.Q., An, H., Yang, F.S., Wang, G.X., Feng, B., Zhang, Z.X. and Rudolph, V. (2012). Modeling of the Carbonation Behavior of a Calcium Based Sorbent for CO_2 Capture. *Int. J. Greenhouse Gas Control.* 10: 510–519.

Received for review, May 25, 2013
Accepted, August 19, 2013